Nanoscale

Accepted Manuscript

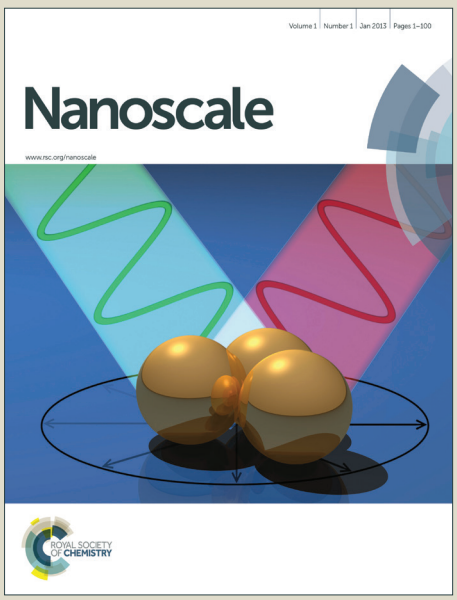

ROYAL SOCIETY OF CHEMISTRY

www.rsc.org/nanoscale

Novel Energy Relay Dyes for High Efficiency Dye-Sensitized Solar Cells

Md. Mahbubur Rahman,[a] Min Jae Ko,[b] and Jae-Joon Lee,[a*]

[a]*Nanotechnology Research Center and Department of Applied Life Science, College of Biomedical and Health Science, Konkuk University, Chungju 380-701, Republic of Korea*

[b]*Photo-Electronic Hybrids Research Center, Korea Institute of Science and Technology (KIST), Seoul 136-791, Republic of Korea*

Abstract

4′,6-Diamidino-2-phenylindole (DAPI) and Hoechst 33342 (H33342) were used as novel energy relay dyes (ERDs) for an efficient energy transfer to N719 dye in I^-/I_3^- based liquid-junction dye-sensitized solar cells (DSSCs). The introduction of the ERDs, either as an additive in the electrolyte or as a co-adsorbent, greatly enhanced the power conversion efficiencies (PCEs), mainly because of an increase of the short-circuit current density (J_{sc}). This was attributed to the effect of the non-radiative Förster-type excitation energy transfer as well as the radiative (emission)-type fluorescent energy transfer to the sensitizers. The net PCEs were 10.65 and 10.57%, an improvement of 12.2 and 11.4% over control devices, for the N719-sensitized DSSCs with DAPI and H33342, respectively.

Keywords: Dye-sensitized solar cell, N719 dye, energy relay dyes, Förster resonance energy transfer, radiative energy transfer.

1. Introduction

The photoelectrode of a dye-sensitized solar cell (DSSC) is principally composed of a mesoporous TiO_2 film covered by a monolayer of light-harvesting dyes.[1-2] DSSCs based on I^-/I_3^- redox mediator with conventional Ru-containing dyes have reached a power conversion efficiency (PCE) of 12%.[3] However, for commercialization, DSSCs must absorb ~ 80% of the solar spectrum (from 350 to 900 nm) and attain a PCE value of 15%. Various strategies have thus been developed to achieve a higher efficiency light harvesting by testing novel dyes, co-sensitizers, and photoelectrode structures as well as the device itself for an effective charge transport and collection.[4-9]

It has been recently demonstrated that the Förster resonance energy transfer (FRET) could be an effective strategy to increase the light harvesting of dyes via a non-radiative transfer of the excited energies from a donor molecule, an energy relay dye (ERD), to an acceptor dye within a short distance range.[10-15] Ideally, higher energy photons absorbed by the donor are efficiently transferred to the acceptor either via a non-radiative FRET or by radiative emission (radiative energy transfer, RET).[10] To achieve this, ERDs must be strongly fluorescent and their emission effectively overlap with the absorption spectra of the acceptor molecules. Several ERDs such as N,N′-di(2,6-diisopropylphenyl)-1,6,7,12-tetra(4-tert-butyl phenyoxy)-perylene-3,4,9,10-tetracarboxylic diimide (PTCDI), tris(4,7-diphenyl-1,10-phenanthroline)ruthenium(II)chloride (N877), 4-dicyanomethylene-2-methyl-6-*p*-dimethylamino-styryl-4*H*-pyran (DCM), 2,2′,7,7′-tetrakis(3-hexyl-5-(7-(4-hexylthiophen-2-yl)benzo[c][1,2,5]tdiazol-4-yl)thiophen-2-yl) 9,9′ spirobifluorene (Spiro-TBT), Rhodamine B (RB), (E)-2-(2-tert-butyl-6-(4-(diethylamino)styryl)-4H-pyran-4-ylidene)malononitrile (BL302), and (E)-2-(2-(2-(5-(4-(bis(2-

ethoxyethyl)amino)phenyl)thiophen-2-yl)vinyl)-6-tert-butyl-4H-pyran-4-ylidene)malononitrile (BL315) have been successfully used to enhance the PCE via FRET for both Spiro-OMETAD based solid-state DSSCs and I^-/I_3^--based liquid-type DSSCs; these were sensitized with squaraine (SQ-1) and zinc-phthalocyanine (TT1), which also functioned as acceptor dyes.[16-21] These ERDs were incorporated into DSSCs by either directly mixing with redox mediators[11,19,29] or blending with the hole-transfer medium (such as Spiro-OMETAD) [17,18] as part of the electrolytes, while they were also introduced as a co-adsorbent along with the sensitizing dyes into the photoelectrode.[20] Although, these ERDs were reported to significantly enhance the overall PCEs in the majority of the previous studies, the ERDs were combined with dyes with a less effective sensitizing capability, such as SQ-1 and TT1-based dyes, which essentially limited the actual PCEs. For instance, the highest cell efficiencies reported for N877 and BL315 with SQ-1 and TT1-based dyes are only 1.80% and 4.14%, respectively.[17,21] It is noteworthy to mention that the co-sensitization of a TiO_2 photoelectrodes by the co-adsorption of two or more molecular sensitizers is another effective strategy to increase the light harvesting efficiency of DSSCs over a wide spectral range.[22-27] Consequently, various co-sensitizing system-based DSSCs have already been developed and suggested the improved PCEs because of the increased light harvesting efficiency.[28-33] In order to enhance light harvesting over a wide wavelength range by both FRET and RET (Figure 1(A)), it is necessary to find commercially available and relatively inexpensive ERDs suitable for the well-known high-efficiency sensitizers such as *cis*-diisothiocyanato-bis(2,2′-bipyridyl-4,4′-dicarboxylato) ruthenium(II) bis(tetrabutylammonium) (N719) and *cis*-bis(isothiocyanato)bis(2,2′-bipyridyl-4,4′-dicarboxylato)-ruthenium(II) (N3). The alkyl-functionalized aminonaphthalimide (carboxy-fluourol, CF) and zinc 2,9,16,23-tetra-*tert*-

butyl-29*H*,31*H*-phthalocyanine (ZnPC-TTB) dyes have been recently used as ERDs for N719 and three different Ru(II) polypyridine complexes (N719, ruthenizer 620-1H3TBA (Black dye) and *cis*-dicyano-bis(2,2′-bipyridyl-4,4′-dicarboxylic acid) ruthenium(II) (Ru505)), respectively,[34,35] however, they showed only limited net enhancement of the quantum efficiency over a narrow spectral range. In this study, we report novel ERDs, namely 4′,6-diamidino-2-phenylindole (DAPI) and Hoechst 33342 (H33342), that ensure a significant enhancement of the net PCEs for sensitizers such as N719, N3, Ru505, and *cis*-disothiocyanato-(2,2′-bipyridyl-4,4′-dicarboxylic acid)-(2,2′-bipyridyl-4,4′-dinonyl) ruthenium(II) (Z907). The contribution of these ERDs to the enhancement of the overall cell efficiency was discussed in terms of the variation of their energy band position, fluorescence quantum yields (Q_d), and Förster radius (R_0) with respect to N719. Finally, the fluorescence quenching of the ERDs induced by N719 and enhancement of the net optical absorption of N719 confirmed the critical role played by the studied ERDs.

2. Results and Discussions

Figure 1(B) shows the chemical structures of DAPI and H33342, which are well-known compounds and often used as DNA-staining agents for fluorescence microscopy; in addition they can absorb high-energy photons.[36,37] The significant overlap of the emission spectra of the ERDs with the absorption spectra of N719 (Figure 1(C)), and the high extinction coefficient (ε) of the ERDs (Table 1) strongly suggest their ability to increase the light harvesting of N719 by non-radiative energy transfer. Furthermore, the intense visible emissions (400–600 nm) of these ERDs indicate the possibility of enhancing the light harvesting of N719 in the visible range via

RET. This is consistent with the relatively high Q_d values calculated for ERDs; such high values may be the result of a favorable R_0[10] between the ERDs and N719 (Table 1, Fig S1; and see the ESI† for further details on these calculations).

These ERDs were incorporated into the DSSCs in two different ways: (i) they were simply mixed with the electrolyte as an additive (**Type-A** cell, designated as ERD|N719/TiO_2, ERD = DAPI or H33342), and (ii) post-adsorbed as a co-adsorbent onto the N719-loaded TiO_2 (N719/TiO_2) surface (**Type-B** cell, designated as ERD-N719/TiO_2, ERD = DAPI or H33342)). For **Type-A** cells, 5 mM of ERD was chosen as the optimum additive concentration (Figure S2); when loaded as a co-adsorbent onto the N719/TiO_2 system, ERDs in ethanolic solutions (1 mM) were used. The current density-voltage (*J-V*) characteristics of both systems under optimized condition are summarized in Figure 2 and Table 2 along with those of the conventional cells sensitized by N719 only. The net PCEs were found to be 10.65% and 10.57% for DAPI|N719/TiO_2 and H33342|N719/TiO_2, respectively; in addition, PCEs were determined to be 10.49% and 10.47% for DAPI-N719/TiO_2 and H33342-N719/TiO_2, respectively, under the fully optimized conditions with a nanocrystalline transparent TiO_2 (20 nm) film (thicknesses of *ca.* 6 μm) and 4-μm thick TiO_2 (500 nm) scattering layer. The net PCEs enhancement compared to the PCEs of cells being sensitized with N719 only was 12.2% and 11.4% for DAPI and H33342, respectively, for **Type-A** cells (DAPI|N719/TiO_2 and H33342|N719/TiO_2); for **Type-B** cells (DAPI-N719/TiO_2 and H33342-N719/TiO_2), these values were determined to be 10.54% and 10.33%. We expect that these ERDs can also be used for cells with other high-efficiency sensitizers, including N3, Ru505, and Z907, because their absorption profiles are similar to that of N719. Indeed, the significant spectral overlap of the absorption of these sensitizers with the

emission profiles of DAPI and H33342 led to PCE enhancement in **Type-A** cells (Figure S3 and Table 2). In this case, the relative PCE enhancement obtained with DAPI and H33342 was 10.4% and 12.5% for N3, 14.0% and 10.9% for Ru505, and 9.3% and 7.0% for Z907, respectively.

The *J-V* and incident-photon-to-current conversion efficiency (IPCE) characteristics of the cells with DAPI/TiO_2 and H33342/TiO_2 shown in the inset of Figures 2(B1-2) and Table 2 (*PCEs* = 0.08% and 0.04 % for DAPI/TiO_2 and H33342/TiO_2, respectively) suggested that the contribution of direct sensitization by DAPI and H33342 is negligible. The low PCE values of DAPI/TiO_2 and H33342/TiO_2 were attributed to the low J_{sc} values, which may result from an inefficient electron injection into the conduction band of TiO_2 (**CB_{TiO2}**) from the highest occupied molecular orbital (HOMO) of both ERDs; this is too positive to interact with **CB_{TiO2}** for a successful electron transfer (Figure 3B and Table 1).[39] The HOMO level and the band gap (*vs.* vacuum) of the ERDs and N719 were calculated from their oxidation potential (*vs.* Ag/Ag^+) obtained from cyclic voltammograms (CVs) (Figure 3A) and absorption onsets (Figure 1B), respectively; these were then used to calculate the lowest unoccupied molecular orbital (LUMO) level of the individual materials.

The cell performance enhancement induced by the ERDs can be mostly attributed to an increase in the J_{sc} values, i.e., up to 7.96% and 6.21% for DAPI|N719/TiO_2 and H33342|N719/TiO_2 (**Type-A**), and 7.63% and 8.34% for DAPI-N719/TiO_2 and H33342-N719/TiO_2 (**Type-B**), respectively. These findings are consistent with the IPCE enhancement observed over the entire wavelength range upon the addition of the ERDs carried out according to both strategies (Figures 2 (A2-B2)). The IPCE in the UV region (*ca.* 340–400 nm) and over a

wide visible range (*ca.* 400–760 nm) was attributed to a non-radiative FRET to N719 occurring around the ERD absorption maxima ($\lambda_{max,\ abs}$ = 348 and 340 nm for DAPI and H33342, respectively) and fluorescent emission-based RET around the ERD emission maxima ($\lambda_{max,\ em}$ = 457 and 460 nm for DAPI and H33342, respectively).

The FRET interaction between the ERDs and N719 is confirmed by the significant quenching of the emission spectra observed for both ERDs as a function of the concentration of N719 (0.2–3 μM), (Figures 4(A-B)); this was done using a similar procedure to that employed in previous studies about the DCM/SQ-1 and Spiro-TBT/TT1 pairs.[18,20] Furthermore, data displayed in Figures 4(C-a) and 4(D-a) show that the amount of light absorption by N719 increases upon incorporation of the ERDs. The significant increase of the net absorption (ΔOD) and effective absorption coefficient (Δα/α) of N719 in the presence of the ERDs over the entire absorption range indicates that the non-radiative and radiative energy transfers contributed simultaneously to the overall light harvesting of N719 (Figures 4C(b-c) & 4D(b-c), in agreement with the previous IPCE increase discussed above. The values of ΔOD and Δα/α showed a maximum at ~ *ca.* 310 nm, close to $\lambda_{max,\ abs}$ of both ERDs; this may be attributed to the FRET interaction between N719 and the ERDs. The increase of ΔOD and Δα/α in the emission maximum region ($\lambda_{max,\ em}$) of the ERDs may be ascribed to the contribution of the increased light intensity due to the fluorescent emission of the ERDs.

Although lower than that of J_{sc}, an increase in open-circuit potential (V_{oc}) was also observed upon introduction of the ERDs; no clear trend in the variation of the fill factor (FF) for N719-based cells was observed. In particular, V_{oc} increased up to *ca.* 28 and 23 mV for DAPI|N719/TiO_2 and H33342|N719/TiO_2 (**Type-A**), and to *ca.* 26 and 10 mV for DAPI-

N719/TiO_2 and H33342-N719/TiO_2 (**Type-B**), respectively. This trend was attributed to the positive shift of the Fermi level of TiO_2 ($\mathbf{E_{F,\ TiO2}}$) because of the basic nature of both ERDs,[40,41] as similarly observed in previous studies on the relationship between V_{oc} and the concentration of basic *tert*-butylpyridine (tBP).[42] The V_{oc} trend observed in this study is also consistent with the recombination rate ($k_{T/E}$) at the photoelectrode/electrolyte interface, which was measured from the Bode plot under the open-circuit and dark conditions for the **Type-A** cells with respect to that of N719/TiO_2 (Figures 5, Table 2).

3. Conclusions

In this work, we have demonstrated that both DAPI and H33342 can be used in combination with most of the high efficiency sensitizers to enhance the efficiency of DSSCs. These ERDs were successfully incorporated into the cells either as a part of the electrolyte or as a co-adsorbent along with the main sensitizer; the net enhancement of the PCE was determined to be *ca.* 12.2% and 11.4% for DAPI and H33342, respectively, with the cells sensitized by N719 under optimum conditions. The increase of J_{sc} was mostly caused by FRET and fluorescent emission-based RET to the sensitizers; in addition the slight increase of V_{oc} was induced by a positive shift of $\mathbf{E_{F,\ TiO2}}$ favored by the basic properties of the ERDs. The application of these materials is expected to be most effective for non-liquid DSSCs and flexible cells that require low-temperature sintering processes; further studies are needed to prove this important point.

Acknowledgements

This research was supported by Basic Science Research Program through the National Research Foundation of Korea (NRF) funded by the Ministry of Education (2013R1A1A4A01013236) and by the New & Renewable Energy Core Technology Program of the Korea Institute of Energy Technology Evaluation and Planning (KETEP) granted financial resource from the Ministry of Trade, Industry & Energy, Republic of Korea (No. 20133030000140). This work was also partly supported by the Center for Inorganic Photovoltaic Materials (2012-0001174) grant funded by the Korea Government (MSIP) and by the National Research Foundation of Korea (NRF) grant funded through the Human Resource Training Project for Regional Innovation.

Notes and References

[a]Nanotechnology Research Center and Department of Applied Life Science, College of Biomedical and Health Science, Konkuk University, Chungju 380-701, Republic of Korea.

[b]Photo-Electronic Hybrids Research Center, Korea Institute of Science and Technology (KIST), Seoul 136-791, Republic of Korea.

[*]To whom correspondence should be addressed. E-mail: jjlee@kku.ac.kr

†Electronic Supplementary Information (ESI†) available: Details of the materials and instrumentation, device fabrication, measurement and calculations of the quantum yield (Q_d), calculations of the Förster radius (R_0), optimization of the ERDs mixed with electrolyte according to **Type-A** strategy; normalized absorption profiles of the N3, Ru505, and Z907 dyes and the emission profiles of DAPI and H33342; *J-V* characteristics of ERD-incorporated DSSCs sensitized with N3, Ru505, and Z907 (**Type-A** strategy). See DOI: 10.1039/C000000x/

1. B. O'Regan and M. Grätzel, *Nature,* 1991, **353**, 737–740.
2. M. J. Ju, I.-Y. Jeon, K. Lim, J. C. Kim, H.-J. Choi, I. T. Choi, Y. K. Eom, Y. J. Kwon, J. Ko, J.-J. Lee, J.-B. Baek and H. K. Kim, *Energy Environ. Sci.*, 2014, **7**, 1044–1052.
3. M. K. Nazeeruddin, F. D. Angelis, S. Fantacci, A. Selloni, G. Viscardi, P. Liska, S. Ito, B. Takeru and M. Grätzel, *J. Am. Chem. Soc.***,** 2005, **127**, 16835–16847.
4. T. W. Hamann, R. A. Jensen, A. B. F. Martinson, H. V. Ryswyk and J. T. Hupp, *Energy Environ. Sci.,* 2008, **1**, 66–78.
5. A. Islam, T. Swetha, M. R. Karim, M. Akhtaruzzaman, L. Han and S. P. Singh, *Phys. Status Solidi A*, 2014, DOI 10.1002/pssa.201431654.
6. M. M. Rahman, N. C. D. Nath, K.-M. Noh, J. C. Kim and J.-J. Lee, *Int. J. Photoenergy*, 2013, Article ID 562130, 1–6.
7. N. C. D. Nath, S. Sarker, A. J. S. Ahammad and J.-J. Lee, *Phys. Chem. Chem. Phys.*, 2012, **14**, 4333–4338.
8. S. Mathew, A. Yella, P. Gao, R. Humphry-Baker, B. F. E. Curchod, N. Ashari-Astani, I. Tavernelli, U. Rothlisberger, M. K. Nazeeruddin and Michael Grätzel, *Nat. Chem.*, 2014, **6**, 242–247
9. M. Yanagida, N. Onozawa-Komatsuzaki, M. Kurashige, K. Sayama and H. Sugihara, *Sol. Energ. Mat. Sol. Cells,* 2010, **94**, 297–302.
10. S. Itzhakov, S. Buhbut, E. Tauber, T. Geiger, A. Zaban and D. Oron, *Adv. Energy Mater.,* 2011, **1**, 626–633.
11. J. I. Basham, G. K. Mor and C. A. Grimes, *ACS Nano,* 2010, **3**, 1253–1258.
12. E. Lee, C. Kim and J. Jang, *Chem. Eur. J.*, 2013, **19**, 10280–10286.

13. J. H. Cheon, S. A. Kim, K.-S. Ahn, M.-S. Kang and J. H. Kim, *Electrochim. Acta*, 2012, **68**, 240–245.

14. N. D. Eisenmenger, K. T. Delaney, V. Ganesan, G. H. Fredrickson and M. L. Chabinyc, *J. Phys. Chem. C*, 2014, **118**, 14098−14106.

15. B. E. Hardin, J.-H. Yum, E. T. Hoke, Y. C. Jun, P. Péchy, T. Torres, M. L. Brongersma, M. K. Nazeeruddin, M. Grätzel and M. D. McGehee, *Nano Lett.*, 2010, **10**, 3077–3083.

16. B. E. Hardin, E. T. Hoke, P. B. Armstrong, J.-H. Yum, P. Comte, T. Torres, J. M. J. Fréchet, M. K. Nazeeruddin, M. Grätzel and M. D. McGehee, *Nat. Photonics,* 2009, **3**, 406–411.

17. J.–H. Yum, B. E. Hardin, S.-J. Moon, E. Baranoff, F. Nüesch, M. D. McGehee, M. Grätzel and M. K. Nazeeruddin, *Angew. Chem. Int. Ed.,* 2009, **48**, 9277 –9280.

18. G. K. Mor, J. Basham, M. Paulose, S. Kim, O. K. Varghese, A. Vaish, S. Yoriya and C. A. Grimes, *Nano Lett.,* 2010, **10**, 2387–2394.

19. J.-H. Yum, B. E. Hardin, E. T. Hoke, E. Baranoff, S. M. Zakeeruddin, M. K. Nazeeruddin, T. Torres, M. D. McGehee and M. Grätzel, *Chem. Phys. Chem.*, 2011, **12**, 657–661.

20. K. Driscoll, J. Fang, N. Humphry-Baker, T. Torres, W. T. S. Huck, H. J. Snaith and R. H. Friend, *Nano Lett.,* 2010**, 10**, 4981–4988.

21. G. Y. Margulis, B. Lim, B. E. Hardin, E. L. Unger, J.-H. Yum, J. M. Feckl, D. Fattakhova-Rohlfing, T. Bein, M. Grätzel, A. Sellinger and M. D. McGehee, *Phys. Chem. Chem. Phys.*, 2013, **15**, 11306–11312.

22. S.-Q. Fan, C. Kim, B. Fang, K.-X. Liao, G.-J. Yang, C.-J. Li, J.-J. Kim and J. Ko, *J. Phys. Chem. C*, 2011, **115**, 7747–7754.

23. J.-H. Yum, S.-R. Jang, P. Walter, T. Geiger, F. Nuesch, S. Kim, J. Ko, M. Grätzel and M. K. Nazeeruddin, *Chem. Commun.*, 2007, **44**, 4680–4682.

24. L. H. Nguyen, H. K. Mulmudi, D. Sabba, S. A. Kulkarni, S. K. Batabyal, K. Nonomura, M. Grätzel and S. G. Mhaisalkar, *Phys. Chem. Chem. Phys.*, 2012, **14**, 16182–16186.

25. J. Mao, F. Guo, W. Ying, W. Wu, J. Li and J. Hua, *Chem. Asian J.*, 2012, **7**, 982–991.

26. S. Paek, H. Choi, C. Kim, N. Cho, S. So, K. Song, M. K. Nazeeruddin and J. Ko, *Chem. Commun.*, 2011, **47**, 2874–2876.

27. C.-M. Lan, H.-P. Wu, T.-Y. Pan, C.-W. Chang, W.-S. Chao, C.-T. Chen, C.-L. Wang, C.-Y. Lin and E. W.-G. Diau, *Energy Environ. Sci.*, 2012, **5**, 6460–6464.

28. . D. Sharma, G. E. Zervaki, P. A. Angaridis, A. Vatikioti, K. S. V. Gupta, T. Gayathri, P. Nagarjuna, S. P. Singh, M. Chandrasekharam, A. Banthiya, K. Bhanuprakash, A. Petrou and A.G. Coutsolelos, *Org. Electron.*, 2014, **15**, 1324–1337.

29. S. P. Singh, M. Chandrasekharam, K. S. V. Gupta, A. Islam, L. Han and G. D. Sharma, *Org. Electron.*, 2013, **14**, 1237–1241.

30. G. D. Sharma, M. S. Roy and S. P. Singh, *J. Mater. Chem.*, 2012, **22**, 18788–18792.

31. G. D. Sharma, D. Daphnomili, K. S. V. Gupta, T. Gayathri, S. P. Singh, P. A. Angaridis, T. N. Kitsopoulos, D. Tasis and A. G. Coutsolelos, *RSC Adv.*, 2013, **3**, 22412–22420.

32. G. D. Sharma, S. P. Singh, P. Nagarjuna, J. A. Mikroyannidis, R. J. Ball and R. Kurchania, *J. Renew. Sustain. Ener.*, 2013, **5**, 043107.

33. G. D. Sharma, S. P. Singh, R. Kurchania and R. J. Ball, *RSC Adv.*, 2013, **3**, 6036–6043.

34. C. Siegers, U. Würfel, M. Zistler, H. Gores, J. Hohl-Ebinger, A. Hinsch and R. Haag, *Chem. Phys. Chem.,* 2008, **9**, 793–798.

35. K. Shankar, X. Feng and C. A. Grimes, *ACS nano*, 2009, **3**, 788–794.

36. P. Chandra, B. Mildner, O. Dann and A. Metz, *Mol. Cell. Biochem.***,** 1977, **18**, 81–86.

37. A. Krishan, *Cytometry*, 1987, **8**, 642-645.

38. P. Wang, C. Klein, R. Humphry-Baker, S. M. Zakeeruddin and M. Grätzel, *J. Am. Chem. Soc.,* 2005, **127**, 808–809.

39. B.-K. An, W. Hu, P. L. Burn and P. Meredith, *J. Phys. Chem. C,* 2010, **114**, 17964–17974.

40. T. Yasujima, K.-Y. Ohta, K. Inoue, M. Ishimaru and H. Yuasa, *Drug Metab. Dispos.*, 2010, **38**, 715–721.

41. J.-Y. Yu, N. Zheng, G. Mane, K. A. Min, J. P. Hinestroza, H. Zhu, K. A. Stringer and G. R. Rosania, *PloS. Comput. Biol*., 2012, **8**, 1–12.

42. S. E. Koops, B. C. O'Regan, P. R. F. Barnes and J. R. Durrant, *J. Am. Chem. Soc.,* 2009, **131**, 4808–4818.

43. J. Qi, X. Dang, P, T. Hammond and A. M. Belcher, *ACS Nano*, 2011, **5**, 7108–7116.

44. T. P. Osedach, N. Zhao, S. M. Geyer, L.-Y. Chang, D. D. Wanger, A. C. Arango, M. C. Bawendi and V. Bulovic, *Adv. Mater.,* 2010, **22**, 5250–5254.

Table 1. Optical parameters of energy relay dyes (ERDs) and N719, energy gap (E_g) and energy band position, quantum yield (Q_d), spectral overlap integral (J), and Försters radius (R_0) along with the available reported values.

Dye / ERDs	$\lambda_{max,abs}$ (nm)	$\lambda_{max,em}$ (nm)	ε ($M^{-1}cm^{-1}$)	E_g (eV)	E_{HOMO} (eV)[a]	E_{LUMO} (eV)[a]	Q_d	J ($M^{-1}cm^3$)	R_o (nm)
N719	380, 517	-	14.0×10^3 [b]	1.80[a], 1.97[b], 1.60 [b]	-5.61	-3.81	-	-	-
DAPI	348	457	2.8×10^4	2.27 [a]	-5.69	-3.42	0.69 [a]	1.22×10^{-15}	2.14
H33342	340	460	4.5×10^4	3.23 [a]	-6.04	-2.81	0.63 [a]	7.37×10^{-16}	1.93

[a] = measured in this research, [b] = reported value [3,38,43]

Table 2. Photovoltaic and kinetic parameters of the different DSSCs cells.

Cells Types	Cells	J_{sc} (mA/cm^2)	V_{oc} (mV)	*FF* (%)	*PCE* (η) (%)	$\Delta\eta / \eta$ (%)[a]	$k_{T/E}$
	$N719/TiO_2$	18.34	717	72.13	9.49		14.0
	$DAPI/TiO_2$	0.11	356	46.59	0.08		
	$H33342/TiO_2$	0.054	364	49.43	0.04		
	$N3/TiO_2$	14.60	704	69.45	7.2		
	$Ru505/TiO_2$	11.95	691	69.0	5.70		
	$Z907/TiO_2$	11.53	675	74.58	5.81		
Type A	$DAPI\|N719/TiO_2$	19.80	745	72.12	10.65	12.2	10.0
	$H33342\|N719/TiO_2$	19.48	740	73.33	10.57	11.4	9.9
	$DAPI\|N3/TiO_2$	15.77	722	69.71	7.95	10.4	
	$H33342\|N3/TiO_2$	16.20	719	69.15	8.10	12.5	
	$DAPI\|Ru505/TiO_2$	13.20	700	70.13	6.50	14.0	
	$H33342\|Ru505/TiO_2$	13.45	697	67.34	6.32	10.9	
	$DAPI\|Z907/TiO_2$	12.45	683	74.58	6.35	9.3	
	$H33342\|Z907/TiO_2$	12.55	678	73.0	6.22	7.0	
Type B	$DAPI\text{-}N719/TiO_2$	19.74	743	71.40	10.49	10.54	
	$H33342\text{-}N719/TiO_2$	19.87	727	72.56	10.47	10.33	

[a] = net enhancement of PCE

Figure Captions

Figure 1. (A) Schematic representation of Förster resonance energy transfer (FRET) and radiative energy transfer (RET) from ERDs to the sensitizing dye, with the ERDs either being (a) mixed with electrolyte (**Type-A**) or (b) co-adsorbed with the dye onto TiO_2 (**Type-B)**. Higher-energy photons absorbed by the ERDs are transferred to the sensitizing dyes either by a direct non-radiative FRET or a radiative emission of lower-energy photons. (B) Chemical structure of DAPI and H33342. (C) Normalized absorption (solid line) and emission (dashed line) profile of (a) DAPI and (b) H33342, together with the absorption profile of N719.

Figure 2. Current density-voltage (*J-V*) plots of DSSCs with the ERDs (A1) added into the I^-/I_3^- based electrolyte and (B1) co-adsorbed onto the N719-loaded TiO_2 surface along with the purely N719-sensitized DSSCs. The corresponding incident-photon-to-current conversion efficiency (IPCE) spectra are displayed in A2 and B2. The insets of B1 and B2 show the *J-V* and IPCE characteristics of the cells sensitized by the ERDs only.

Figure 3. (A) Cyclic voltammograms (CVs) of N719, DAPI, H33342 in an MPN solution containing 0.1 M tetrabutylammonium tetrafluoroborate as the supporting electrolyte; scan rate: 100 mV/s. (B) Energy-level alignment of DAPI, H33342, N719, TiO_2, along with the redox potential of I^-/I_3^-.

Figure 4: Emission spectra of (A) DAPI and (B) H33342 (0.02 μM, respectively)-only (red) and the quenching of their emission in the presence of N719 up to 3 μM. (C-D): (a) Enhancement of light absorption of N719 in the presence of the ERDs in the MPN solution (the concentrations of DAPI, H33342, and N719 are 10, 20, and 8 μM, respectively); (b) the net absorption change

(ΔOD) of N719 and (c) relative changes of the effective absorption coefficient (Δα/α) were measured according to a published procedure.[44]

Figure 5: Bode plots from the EIS measurement of DSSCs under dark and open-circuit conditions.

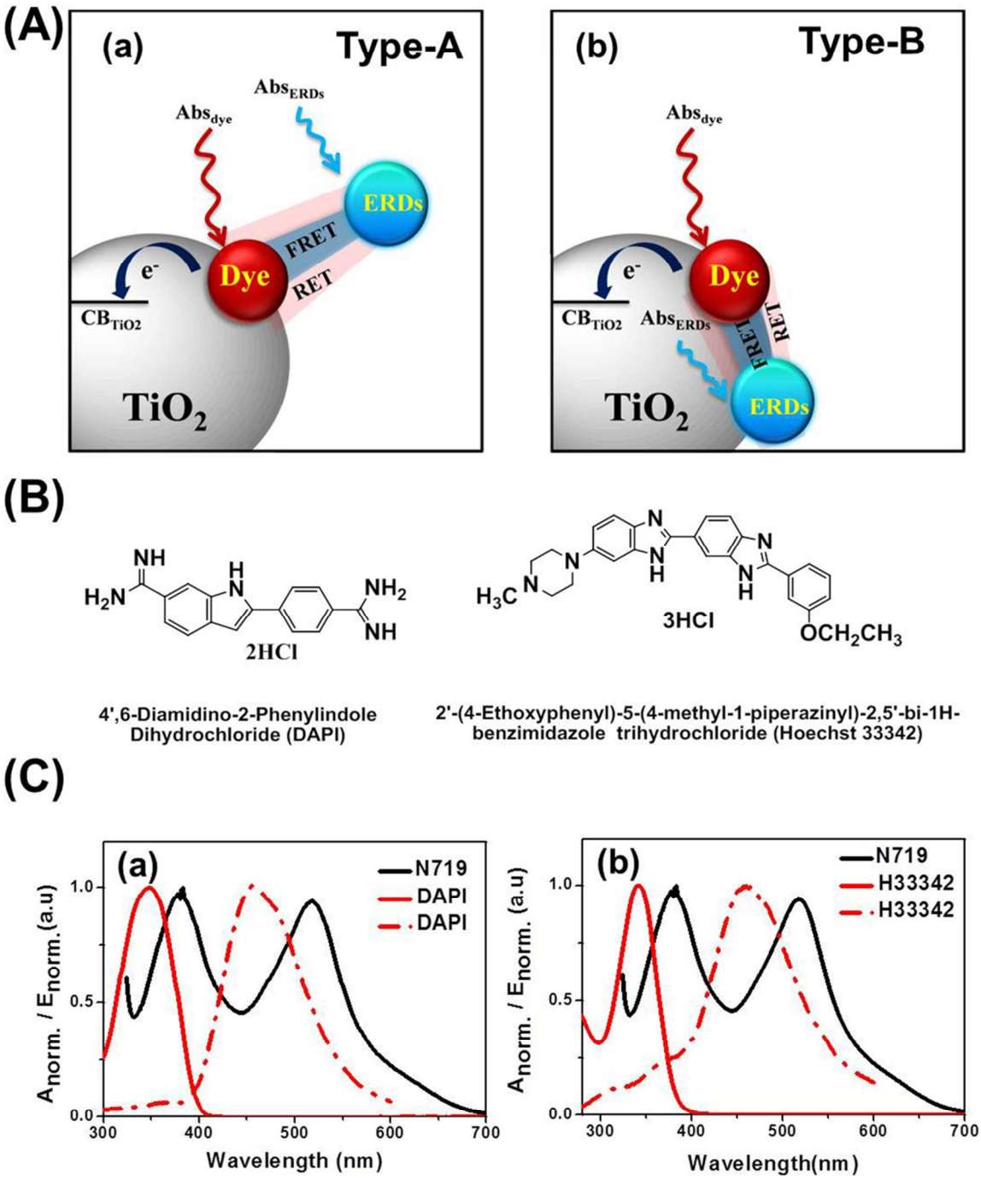

Figure 1: J.-J. Lee et al.

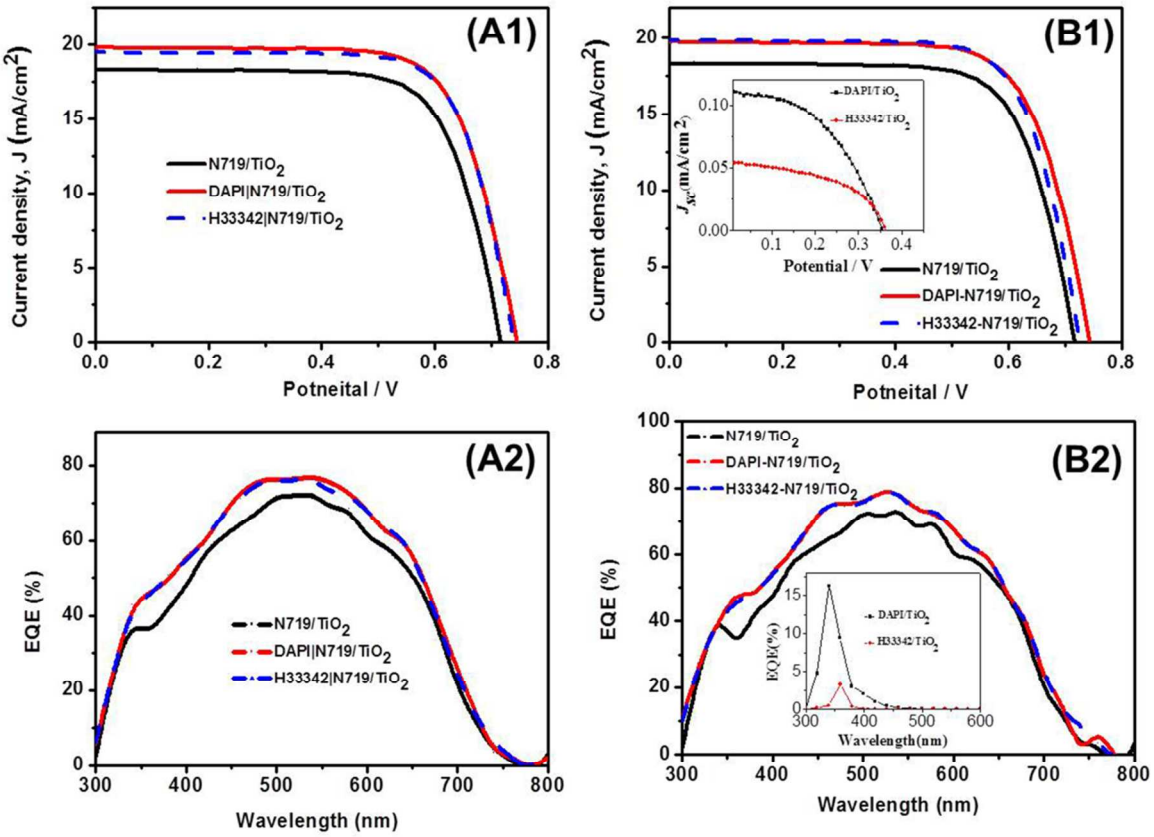

Figure 2: J.-J. Lee et al.

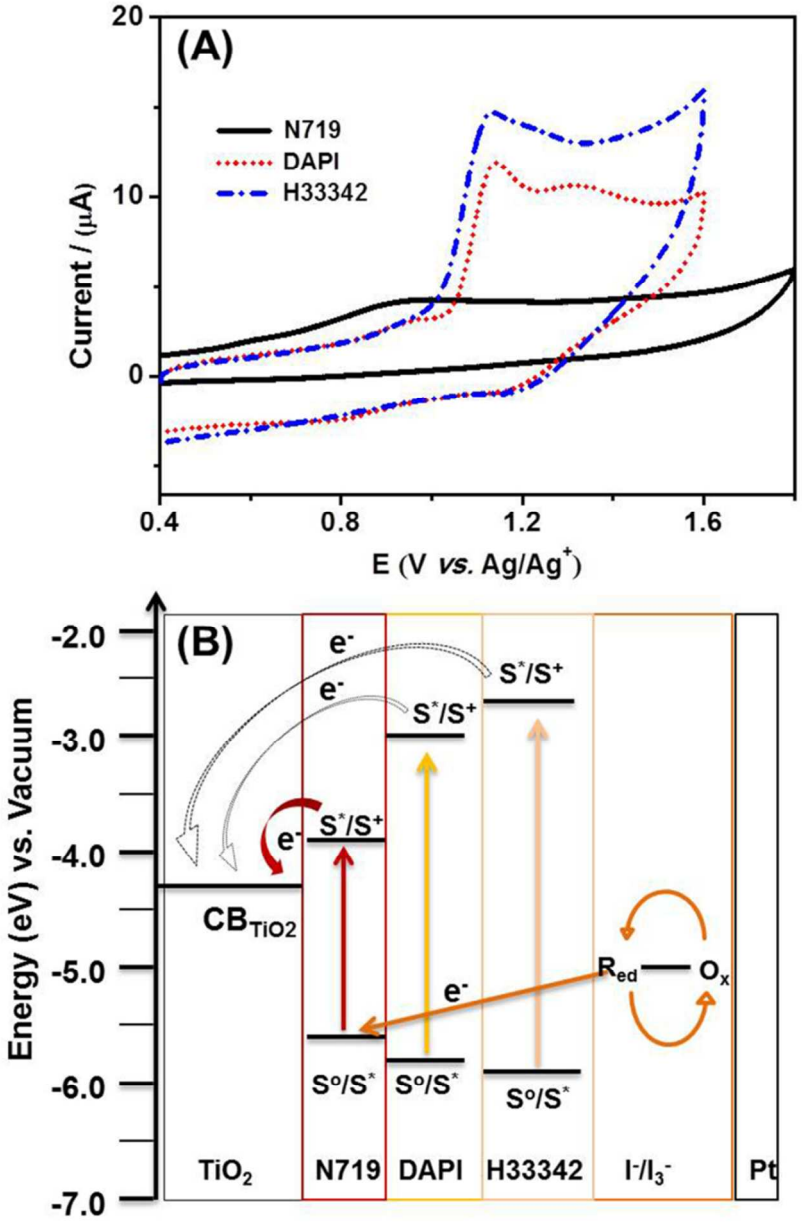

Figure 3: J.-J. Lee et al.

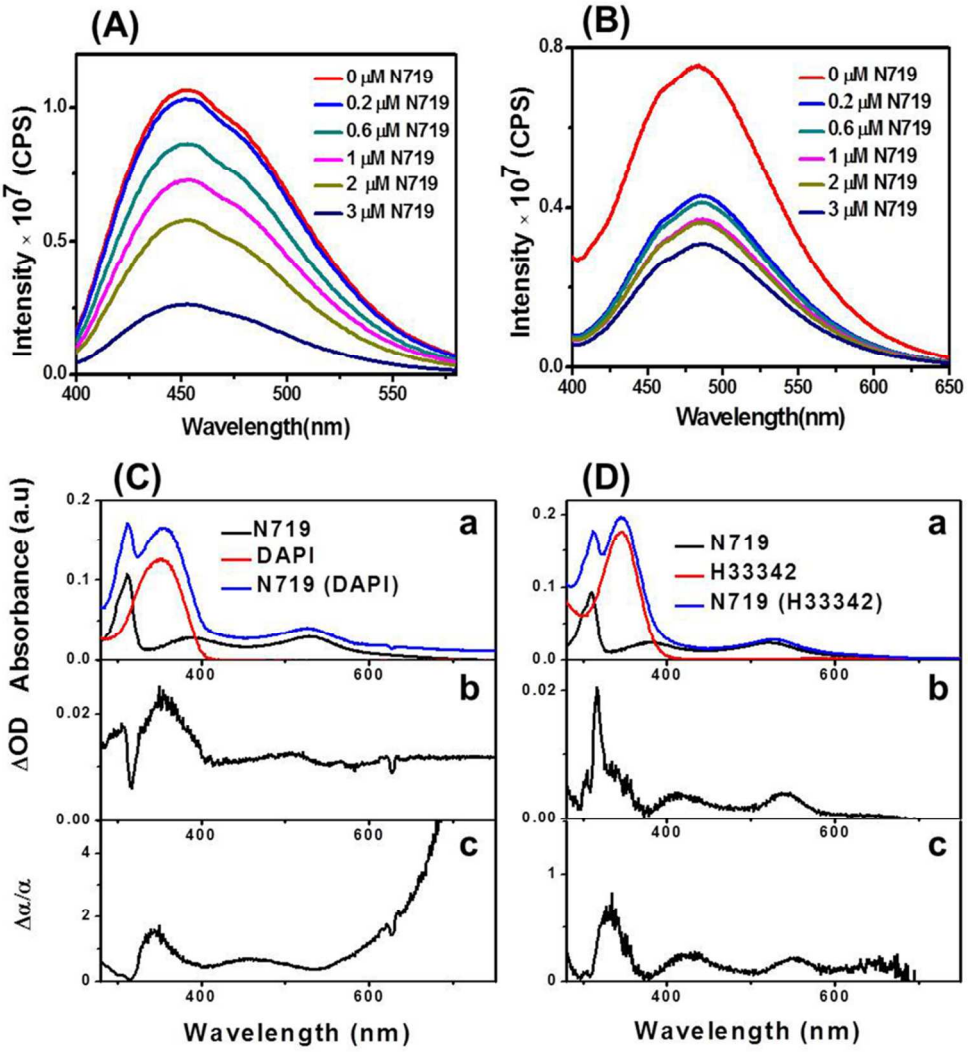

Figure 4: J.-J. Lee et al.

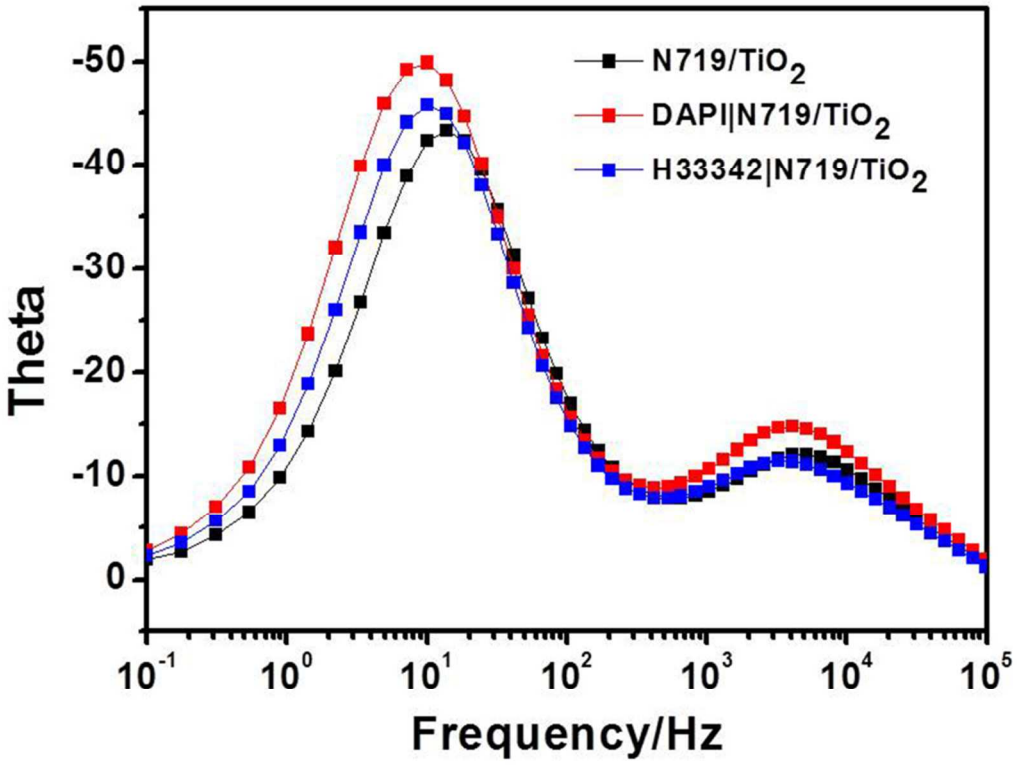

Figure 5: J.-J. Lee et al.